

AD-A172 817

RAMAN ISOSBESTIC POINTS FROM WATER(U) HOWARD UNIV  
WASHINGTON DC DEPT OF CHEMISTRY G E MALRAVEN ET AL.  
OCT 86 TR-24-ONR N00014-86-C-8305

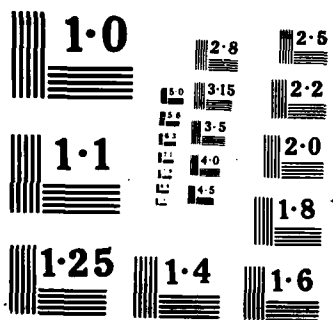
1/1

UNCLASSIFIED

F/G 7/4

NL

END  
DATE  
FILMED  
11 1986  
DTIC



AD-A172 817

(12)

Unclassified

ORIGINAL CLASSIFICATION OF THIS PAGE

## REPORT DOCUMENTATION PAGE

REPORT SECURITY CLASSIFICATION Unclassified		1b. RESTRICTIVE MARKINGS	
SECURITY CLASSIFICATION AUTHORITY		3. DISTRIBUTION/AVAILABILITY OF REPORT	
DECLASSIFICATION/DOWNGRADING SCHEDULE		Unrestricted	
PERFORMING ORGANIZATION REPORT NUMBER(S) ONR-TR-24		5. MONITORING ORGANIZATION REPORT NUMBER(S)	
NAME OF PERFORMING ORGANIZATION Howard University Department of Chemistry	6b. OFFICE SYMBOL (If applicable)	7a. NAME OF MONITORING ORGANIZATION Office of Naval Research Chemistry Division	
ADDRESS (City, State, and ZIP Code) 1000 College Street, NW Washington, DC 20059		7b. ADDRESS (City, State, and ZIP Code) Arlington, Virginia 22217-5000	
NAME OF FUNDING/SPONSORING ORGANIZATION	8b. OFFICE SYMBOL (If applicable)	9. PROCUREMENT INSTRUMENT IDENTIFICATION NUMBER N00014-80-C-0305	
ADDRESS (City, State, and ZIP Code)		10. SOURCE OF FUNDING NUMBERS	
		PROGRAM ELEMENT NO.	PROJECT NO.
		TASK NO.	WORK UNIT ACCESSION NO.
TITLE (Include Security Classification) Raman isosbestic points from water			
PERSONAL AUTHOR(S) Walrafen, G.E., Hokmabadi, M. S. and Yang, W. H.-			
TYPE OF REPORT Technical	13b. TIME COVERED FROM 3/86 to 10/86	14. DATE OF REPORT (Year, Month, Day) 86-10-03	15. PAGE COUNT 8
SUPPLEMENTARY NOTATION			
COSATI CODES		18. SUBJECT TERMS (Continue on reverse if necessary and identify by block number)	
FIELD	GROUP	SUB-GROUP	
		Raman, water, isosbestic points	
ABSTRACT (Continue on reverse if necessary and identify by block number)			
Precise isosbestic points of water have been measured in the OH stretching region of the Raman spectrum. Measurements were carried out between 3 and 85 °C and for several orientations.			
<div style="display: flex; justify-content: space-around; align-items: center;"> <div style="text-align: center;"> <p>DTIC FILE COPY</p> </div> <div style="text-align: center;"> <p>DTIC ELECTE OCT 08 1986</p> </div> </div>			
DISTRIBUTION/AVAILABILITY OF ABSTRACT <input checked="" type="checkbox"/> UNCLASSIFIED/UNLIMITED <input type="checkbox"/> SAME AS RPT. <input type="checkbox"/> DTIC USERS		21. ABSTRACT SECURITY CLASSIFICATION Unclassified	
NAME OF RESPONSIBLE INDIVIDUAL G. E. Walrafen		22b. TELEPHONE (Include Area Code) 202-636-6897	22c. OFFICE SYMBOL

OFFICE OF NAVAL RESEARCH

Contract N00014-80-C-0305

R & T Code 4131023

TECHNICAL REPORT NO. 24

Raman isosbestic points from water

by

G. E. Walrafen, M. S. Hokamabadi, and W. H.-Yang

to be published in the Journal of Chemical Physics

Department of Chemistry  
Howard University  
Washington, DC 20059

Reproduction in whole, or in part is permitted for any  
purpose of the United States Government.

\* This document has been approved for public release and  
sale; its distribution is unlimited

Running Title: Isosbestic points from water

## Raman isosbestic points from water

G. E. Walrafen, M. S. Hokmabadi, and W. -H. Yang<sup>a)</sup>

Department of Chemistry, Howard University, Washington, D.C. 20059

(Received 7 July 1986; accepted 31 July 1986)

Precise isosbestic points occur in the Raman OH-stretching spectra from liquid water between 3 and 85 °C if cell alignment is accomplished with Newton's rings. Isosbestic frequencies measured for the orientations  $X(Y, X + Z)Y = 6\beta^2$ ,  $X(ZX)Y = 3\beta^2$ ,  $X(Y + Z, X + Z)Y = 45\alpha^2 + 13\beta^2$ ,  $X(Z, X + Z)Y = 45\alpha^2 + 7\beta^2$ , and  $X(ZZ)Y = 45\alpha^2 + 4\beta^2$  are 3524, 3522 (note  $\beta^2$  agreement), 3468, 3425, and 3403  $\text{cm}^{-1}$ , respectively. Isosbestic points from two different measurements calculated by the relations,  $X(ZZ)Y - (4/3)X(ZX)Y$  and  $X(Z, X + Z)Y - (7/6)X(Y, X + Z)Y$  agree exactly for  $45\alpha^2$ , 3370  $\text{cm}^{-1}$ . ( $\alpha$  and  $\beta^2$  correspond to the mean polarizability and square of the anisotropy.) The pure  $\alpha^2$  isosbestic frequency, 3370  $\text{cm}^{-1}$ , coincides with the peak of the highest frequency hydrogen-bonded (HB) Gaussian OH-stretching component. The pure  $\beta^2$  isosbestic point, 3522–3524  $\text{cm}^{-1}$ , coincides with the peak of the nonhydrogen-bonded (NHB) Gaussian OH-stretching component, next above in frequency. The  $\alpha^2$  and  $\beta^2$  isosbestic points are thus thought to provide an experimental distinction between, and a clear definition of, the HB and NHB OH-oscillator classes for water. Moreover, the various OH-stretching combinations of  $\alpha^2$  and  $\beta^2$  simply provide different measures of the HB→NHB equilibrium—no special information concerning the temperature dependence of this equilibrium results from use of any one linear polarizability combination over any other, including pure  $\alpha^2$  or pure  $\beta^2$ . The present results agree with mercury-excited data [Walrafen, *J. Chem. Phys.* **47**, 114 (1967)] for  $X(Y + Z, X + Z)Y$  and with the corrected  $\alpha^2$  data of d'Arrigo *et al.* [*J. Chem. Phys.* **75**, 4264 (1981)]. Furthermore, the new data are in accord with the spectroscopic mixture model, but the continuum model conflicts with the observation of exact points. The isosbestic frequencies are also found to be strongly nonlinear in the amount of  $\alpha^2$  or  $\beta^2$  involved in the spectra.

## I. INTRODUCTION

The term "isosbestic" point was used at least as early as 1924 by Thiel.<sup>1</sup> It refers to the wavelength at which a series of absorption spectra cross, i.e., where the absorbance is a constant. To give a specific example, the visible absorption spectrum from bromophenol blue displays an exact isosbestic point just above a wavelength of 5000 Å when the pH of the solution is varied from 2.6 to 5.4.<sup>1,2</sup> In this case a plot of the absorbance at the isosbestic wavelength vs pH is a straight line parallel to the pH axis.

The appropriate term for Raman scattering is "isoskedastic" (equal scattering) point.<sup>3</sup> However, isosbestic point is used here. At the isosbestic point, the scattered intensity under constant excitation power, and at a fixed Raman frequency,  $\Delta\bar{\nu} \text{ cm}^{-1}$ , is constant and independent of the intensive quantity, e.g., temperature, concentration, that gives rise to the spectral changes, for the pure liquid or solution studied.

The existence of an isosbestic point in a liquid or solution may mean that the peaks of the spectral bands are constant in position (and in component shape and half-width), and change only in intensity. Moreover, if the point is exact, the presence of an equilibrium between two absorbers or scatterers may be inferred.<sup>4</sup> An exact isosbestic point can be shown to arise from conservation of species concentration; and, of absorbance or Raman scattering, as seen next.

Consider the simplest possible case illustrated by Eqs. (1) and (2). (For more complex situations and caveats see

Refs. 5–10.) A and B of Eqs. (1) and (2) refer to two forms, species, or classes of interaction.  $\chi$  refers to either absorbance or absolute Raman intensity, and  $J_A$  and  $J_B$  refer to values of the corresponding (molar) coefficients at the isosbestic point *only*. (The product of thickness and molar absorptivity is involved in the  $J$ 's for the absorption case.)

$$[A] + [B] = \text{const}, \quad (1)$$

and

$$\chi = J_A [A] + J_B [B]. \quad (2)$$

Differentiation of Eqs. (1) and (2) with respect to the appropriate intensive variable  $\Omega$ , e.g., pH, temperature, concentration, pressure, time, which produces the spectral changes (without changes in component position, half-width, or shape) yields

$$\frac{d[A]}{d\Omega} = -\frac{d[B]}{d\Omega}, \quad (3)$$

and

$$\frac{J_A d[A]}{d\Omega} + \frac{J_B d[B]}{d\Omega} = \frac{d\chi}{d\Omega}. \quad (4)$$

But  $d\chi/d\Omega$  is zero at the isosbestic point, and  $[A]$  and  $[B]$  must change continuously with  $\Omega$ , i.e.,  $d[A]/d\Omega \neq 0$  and  $d[B]/d\Omega \neq 0$ . Hence,

$$J_A = J_B. \quad (5)$$

The equality (5) refers to the fact that the molar Raman intensity or in absorption, the molar absorptivity—thickness product, is the same for both A and B at the isosbestic point.

<sup>a)</sup> Institute of Physics, Chinese Academy of Science, Beijing, China.

Worley and Klotz<sup>11</sup> were probably the first workers to attract wide attention to isosbestic points for water. They combined information from isosbestic points with thermodynamic analysis of infrared overtone bands to obtain consistent  $\Delta H^\circ$  values for bonded to nonbonded (HB $\rightarrow$ NHB) equilibria between uncoupled HDO oscillators. Later, Walrafen reported exact Raman isosbestic points for pure water,  $3460 \pm 5 \text{ cm}^{-1}$ ,<sup>12</sup> and for the OD-stretching region of HDO in  $\text{H}_2\text{O}$ ,  $2570 \pm 5 \text{ cm}^{-1}$ .<sup>13</sup> See also Ref. 14. Scherer *et al.*,<sup>15</sup> however, subsequently contested Walrafen's mercury-excited results,<sup>12</sup> and contended that isosbestic points were absent in the pure  $\alpha^2$  spectra from both liquid  $\text{H}_2\text{O}$  and  $\text{D}_2\text{O}$ . But d'Arrigo *et al.*<sup>16</sup> recently repeated Scherer's data and demonstrated an isosbestic point at  $3370 \text{ cm}^{-1}$  in the pure  $\alpha^2$  spectra from  $\text{H}_2\text{O}$ . Unfortunately, d'Arrigo *et al.* obtained their isosbestic point by refractive index correction, and this may have cast doubt upon its exactness. For example, a very recent review<sup>17</sup> highlighted the erroneous results of Scherer *et al.*

In the present work exactly defined isosbestic points were found for pure water under seven different experimental conditions<sup>18</sup> plus the two separate determinations of the  $45\alpha^2$  isosbestic point which agreed exactly,  $3370 \text{ cm}^{-1}$ . Furthermore, the present  $45\alpha^2$  isosbestic frequency is identical to that reported by d'Arrigo *et al.*, but the present point was found directly from the raw data. No corrections whatever were needed to obtain it.

A method of cell alignment employing Newton's rings was used.<sup>19</sup> With this method exact isosbestic points resulted directly. Without it (when Newton's rings were lacking) crossing phenomena indistinguishable from those reported by Scherer *et al.* were seen. The problem involves the strong temperature dependence of the refractive index of water.<sup>20</sup> When the (horizontal) laser beam is not exactly perpendicular to the (side) window of the Raman cell, it is continuously bent as the refractive index changes. In an extreme case, used only for illustration, one can envision the laser beam crossing the (horizontal) slit at a very steep angle at one temperature, but parallel to the slit at another temperature. The result is that the number of Raman photons collected in the two cases varies according to the ratio of the common laser beam and slit areas, with the production of large errors in intensity. In fact, it has been established here that the errors resulting from the use of ordinary mensuration to determine 90 deg incidence can be sufficient to preclude the observation of exact points. Without precisely defined 90 deg incidence, as obtained with Newton's rings, one may simply be monitoring the temperature dependence of the refractive index of water by means of the Raman intensity change.

The new Raman isosbestic points, and the experimental method used to obtain them, are described next.

## II. EXPERIMENTAL PROCEDURES

Details of the Raman instrumentation, the Raman cell, temperature control and measurement, water purification, etc., are described in the following article.<sup>19</sup> The optical alignment and polarization methods are described here.

The laser beam position in the water was held precisely fixed at all temperatures by use of Newton's rings and auxiliary measurements. Newton's rings were observed from the backward reflection of the laser beam 3 m from the entrance (side) window of the Raman cell. The position of the laser beam emitted from the exit window was also determined simultaneously by use of a hole 3 m away. At a series of temperature from 3 to 85 °C, no change in Newton's rings was seen, and no change in the exit beam position occurred. Hence, no bending of the beam in the water was possible as the refractive index of the water changed. Moreover, the fused silica cell windows were chosen for their precisely parallel faces, and these windows rested directly on precisely machined, parallel surfaces of the stainless steel Raman cell.

For the polarization geometries  $X(ZZ)Y$  and  $X(ZX)Y$ , a polaroid plate was rotated by exactly 90 deg in front of the (horizontal) slit. A polarization scrambler was used between the slit and the polaroid. The electric vector of the laser beam was maintained in the vertical  $Z$  direction for both geometries.

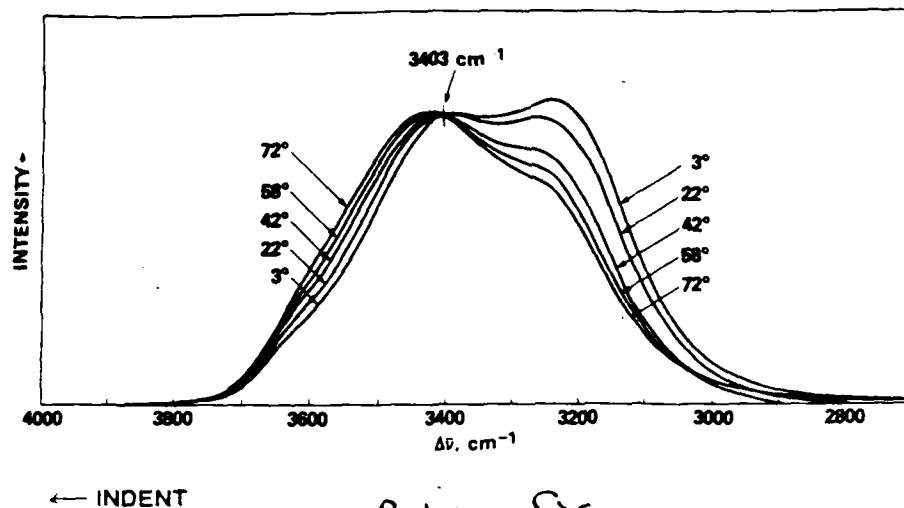
For the  $X(ZX + Z)Y$  and  $X(YX + Z)Y$  measurements, the electric vector of the laser beam was rotated exactly 90 deg from the vertical  $Z$  position to the horizontal  $Y$  position. The polaroid plate was omitted and only the polarization scrambler was used in front of the slit.

For the completely unpolarized case,  $X(Y + ZX + Z)Y$ , unpolarized laser light was required. The laser beam was first expanded, passed through a polarization scrambler, and then condensed before passage into the Raman cell. Alternatively, unpolarized laser light was produced by passage through 10 m of a 200  $\mu\text{m}$  diameter fused silica multimode optical fiber coiled in loops of about 10 cm radius. The output of the fiber was formed into a parallel beam about 1 mm wide, and passed through the Raman cell. Newton's rings were observed in both cases.

Measurements involving the  $X(ZX + Z)Y$  and  $X(YX + Z)Y$  orientations were also made without using a scrambler in front of the slit.<sup>18</sup> These measurements may be viewed as yielding other linear combinations of  $\alpha^2$  and  $\beta^2$  because the grating response is considerably different for the vertical and horizontal polarizations. From  $X(ZX + Z)Y$ ,  $X(YX + Z)Y$ , and  $X(ZX + Z)Y - (7/6)X(YX + Z)Y$  three additional exact isosbestic points at 3396, 3510, and  $3363 \text{ cm}^{-1}$  ( $45 \alpha^2$ ), respectively, resulted for spectra between 3 and 72 °C. These results are not shown here.

The collection angle involved in this work at 90 deg to the laser beam, the  $Y$  direction, using a 40 cm collection lens was only a few degrees. Nevertheless, changes of refractive index can, in principle, produce intensity errors here as well. To test the refractive index effect in the  $Y$  direction, a single 0.5 mm diameter pin hole was placed in front of the collection window of the Raman cell 60 mm from the laser beam ( $X$  direction). This yielded a solid collection angle of  $6 \times 10^{-5} \text{ sr}$ . For the  $X(ZX + Z)Y$  geometry, and without using a polarization scrambler, an isosbestic frequency of  $3396 \text{ cm}^{-1}$  resulted in exact agreement with the corresponding uncollimated result. No measurable error thus results from refractive index effects in the  $Y$  direction.

## LIMIT OF TEST



Retype Fig.  
CAP 42.5

- INDENT

between 3 and 72 °C for the orientation  $X(ZZ)Y$ .  $X$  is the (horizontal) laser beam direction, and  $Y$  is the (horizontal) observation direction, 90 deg scattering. The first letter in parentheses refers to the direction,  $Z$  (vertical), of the electric vector of the laser beam, and the second letter to the direction of the electric vector of the Raman radiation. A polarization scrambler was used for all spectra shown here. Figs. 1-6. No adjustment of spectral ordinates was carried out in this or in the following five figures i.e., the spectral amplitudes coincide exactly at 3800  $\text{cm}^{-1}$ . The isosbestic point at 3403  $\text{cm}^{-1}$  is indicated by the bar in this and all following spectra. All isosbestic frequency values were determined from the original, large strip chart recordings.

### III. EXPERIMENTAL RESULTS

#### A. Polarized and depolarized spectra

Absolute Raman spectra (intensities quantitatively comparable) are shown for the  $X(ZZ)Y$  and  $X(ZX)Y$  orientations in Figs. 1 and 2. Exact isosbestic points are seen in the figures at 3403 and 3522  $\text{cm}^{-1}$  which correspond to  $45\alpha^2 + 4\beta^2$  and to  $3\beta^2$ , respectively. Furthermore, Fig. 3(a) shows  $X(ZZ)Y - (4/3)X(ZX)Y = 45\alpha^2$ , where an exact isosbestic point occurs at 3370  $\text{cm}^{-1}$ . This result is identical to the corrected result of d'Arrigo *et al.*<sup>16</sup>

Figures 4 and 5 show spectra corresponding to the  $X(Z,X + Z)Y$  and  $X(Y,X + Z)Y$  orientations. Exact isosbestic points occur at 3425 and 3524  $\text{cm}^{-1}$  which correspond to  $45\alpha^2 + 7\beta^2$  and to  $6\beta^2$ , respectively. The  $6\beta^2$  isosbestic frequency agrees with the  $3\beta^2$  value within 2  $\text{cm}^{-1}$ , or 0.06%. (The isosbestic frequency in this case is independent of the multiplier, i.e., 3 or 6.) The  $45\alpha^2$  spectra that result from  $X(Z,X + Z)Y - (7/6)X(Y,X + Z)Y$  are shown in Fig. 3(b), where exact agreement with Fig. 3(a) occurs for the isosbestic point, 3370  $\text{cm}^{-1}$ .

#### B. Unpolarized spectra

Absolute Raman spectra are shown in Fig. 6 for the totally unpolarized case  $X(Y + Z,X + Z)Y$ . An exact isosbestic point occurs at 3468  $\text{cm}^{-1}$  in the figure. Figure 6 spectra correspond to  $45\alpha^2 + 13\beta^2$ , and the present isosbestic frequency agrees well with the totally unpolarized mercury-excited value of  $3460 \pm 5 \text{ cm}^{-1}$  reported 20 years ago by Walrafen.<sup>12</sup> Scherer *et al.*, however, did not measure this point, but rather calculated a value of 3475  $\text{cm}^{-1}$  for it from  $45\alpha^2 + 13\beta^2$ . However, their data were in error and failed to show an isosbestic point in either  $45\alpha^2$  or  $4\beta^2$ . They concluded, therefore, that any exact isosbestic point in  $45\alpha^2 + 13\beta^2$  would have to result from cancellation effects. But, this conclusion is incorrect as seen from the fact that both the present laser-excited and the previous mercury-excited spectra show exact isosbestic points.<sup>21</sup>

#### C. Nonlinear dependence of isosbestic frequency upon $\alpha^2$ and $\beta^2$ .

In Fig. 7 isosbestic frequencies,  $\Delta\nu_{\text{ISOS}}$ , measured here, are plotted against the fraction of  $\beta^2$ ,  $f(\beta^2) = b/(a + b)$ .

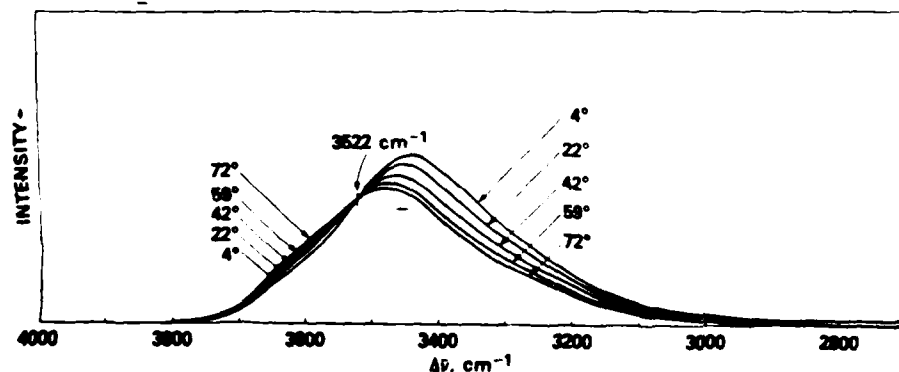


FIG. 2. Absolute Raman spectra in the OH-stretching region from water between 4 and 72 °C for the orientation  $X(ZX)Y$ . All intensities are increased by a factor of  $\sim 2.5$  relative to Fig. 1. Isosbestic point 3522  $\text{cm}^{-1}$ .

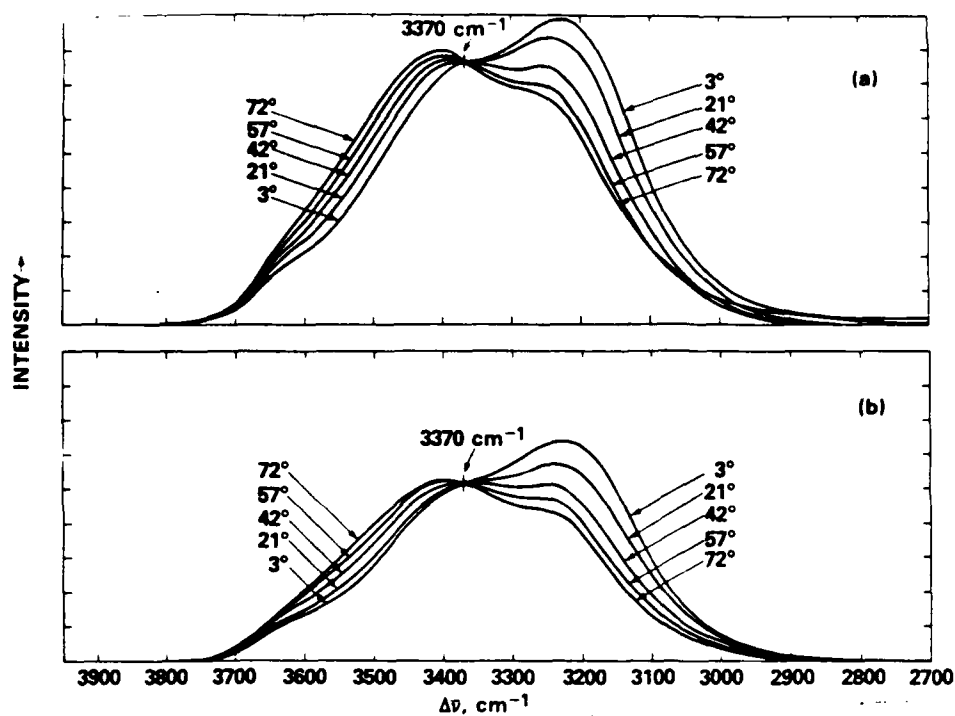


FIG. 3. Isotropic Raman spectra from water between 3 and 72 °C. (a) refers to  $X(ZZ)Y - (4/3)X(ZX)Y = 45a^2$ , and (b) refers to  $X(Z,X+Z)Y - (7/6)X(Y,X+Z)Y = 45a^2$ . (a) intensities are increased relative to the (b) intensities, e.g., the scaling factor is evident at 3370  $\text{cm}^{-1}$ , the isosbestic point.

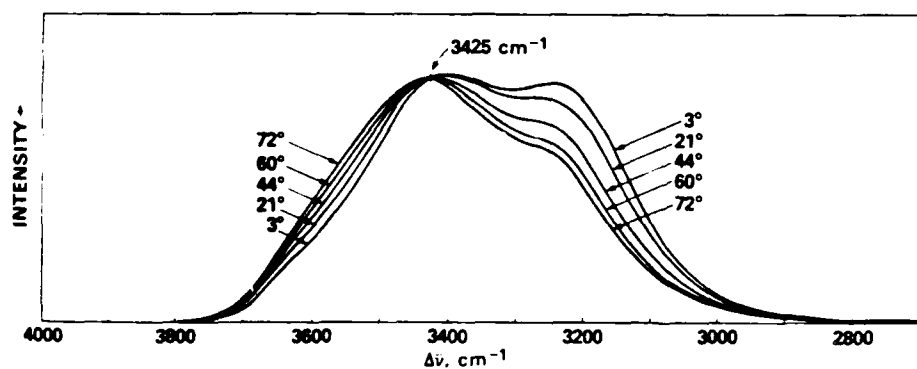


FIG. 4. Absolute Raman spectra in the OH-stretching region from water between 3 and 72 °C for the orientation  $X(Z,X+Z)Y$ .  $X+Z$  means that both the  $X$  and  $Z$  polarizations of the Raman scattering were collected. Isosbestic point, 3425  $\text{cm}^{-1}$ .

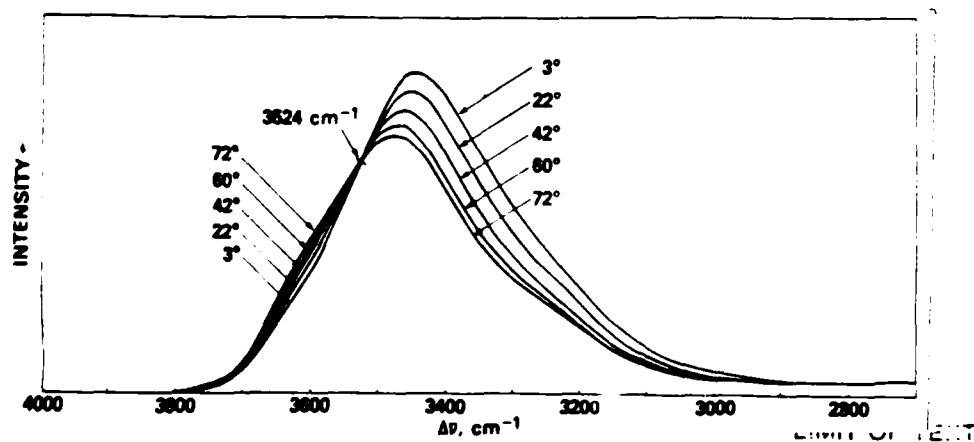


FIG. 5. Absolute Raman spectra in the OH-stretching region from water between 3 and 72 °C for the orientation  $X(Y,X+Z)Y$ . All intensities are increased by a factor of  $\sim 3.6$  relative to Fig. 4. Isosbestic point, 3524  $\text{cm}^{-1}$ .



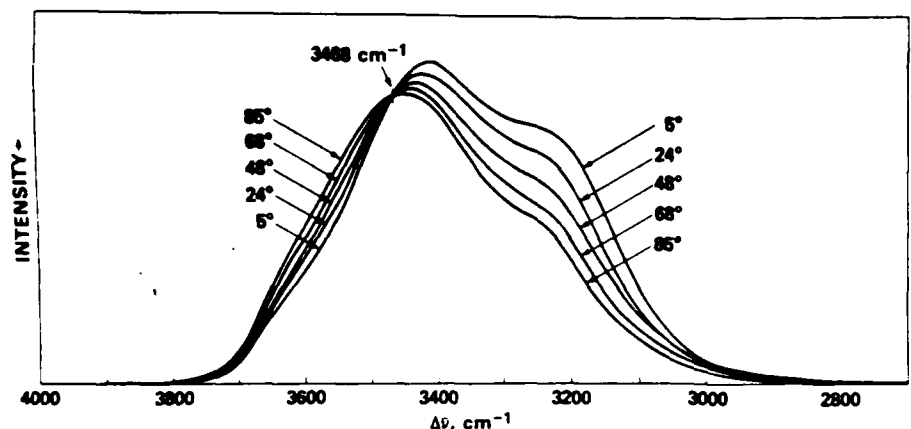


FIG. 6. Absolute Raman spectra in the OH-stretching region from water between 5 and 85 °C for the completely unpolarized excitation and detection case  $X(Y + Z, X + Z)Y$ . Unpolarized laser light was obtained using an optical fiber, see Sec. II. Isosbestic point, 3468  $\text{cm}^{-1}$ .

where  $b$  is the  $\beta^2$  coefficient in a given spectrum, and  $a$  is the  $\alpha^2$  coefficient.  $\Delta\nu_{\text{ISOS}}$  is seen to be strongly nonlinear in  $f(\beta^2)$ . For the completely unpolarized case, the calculated  $\Delta\nu_{\text{ISOS}}$  of Scherer *et al.* lies well above the curve in the figure. The mercury-excited value of Walrafen<sup>12</sup> lies on the curve, and the present unpolarized laser-excited value slightly above. If the isosbestic frequency of 3396  $\text{cm}^{-1}$  obtained without a scrambler for the  $X(Z, X + Y)Y$  orientation is placed on the curve to determine the corresponding  $f(\beta^2)$ , the  $f(\beta^2)$  value that results is less than that calculated from

$45\alpha^2 + 7\beta^2$ . The extra  $\alpha^2$  contribution arises from the polarization response of the holographic gratings of the J.-Y. HG 2S instrument used here.<sup>22</sup> Two calculated isosbestic frequencies corresponding to  $45\alpha^2 + 45\beta^2$  and  $45\alpha^2 + 135\beta^2$  are also included in Fig. 7. In this regard, it should be emphasized that it is possible in principle to calculate any linear combination of  $\alpha^2$  or  $\beta^2$ . However, if errors occur in either of the  $\alpha^2$  or  $\beta^2$  spectra,<sup>15</sup> these errors will be carried into the calculated spectra. Therefore, the various measurements of this work are not redundant. On the contrary, they are absolutely necessary to test the accuracy of the data.

#### D. Relation to Gaussian components

Walrafen<sup>23</sup> has reported the results of Gaussian analysis of the  $3\beta^2$ ,  $45\alpha^2$ , and  $45\alpha^2 + 4\beta^2$  Raman OH-stretching contours from water. For the  $45\alpha^2$  spectrum, the Gaussian component peak positions are: (1) 3110  $\text{cm}^{-1}$ , (2) 3212  $\text{cm}^{-1}$ , (3) 3383  $\text{cm}^{-1}$ , (4) 3520  $\text{cm}^{-1}$ , and (5) 3620  $\text{cm}^{-1}$ . The present pure  $\alpha^2$  isosbestic frequency, 3370  $\text{cm}^{-1}$ , corresponds to component (3), which is the highest-frequency HB component, as seen from decrease of intensity with temperature rise.<sup>12</sup> The present  $\beta^2$  isosbestic frequency 3522–3524  $\text{cm}^{-1}$ , corresponds to component (4), which is the next component above in frequency, and which, from its opposite temperature dependence, is an NHB component.<sup>12</sup> Hence, it is thought that the pure  $\alpha^2$  isosbestic frequency accurately defines the upper frequency limit for the peak position of the HB components, and that the pure  $\beta^2$  isosbestic frequency accurately defines the lower frequency limit for the peak position of the NHB components. Alternatively, the frequency region between the pure  $\alpha^2$  and pure  $\beta^2$  isosbestic frequencies, is thought to define the transitional region from hydrogen-bonded to nonhydrogen-bonded interactions.

#### E. Relation to models of water structure

Advocates of the continuum model of water structure have long claimed that the lack of isosbestic points in the Raman spectra from water is evidence for their model (cf. Ref. 15). From the present work, however, it is unmistakably clear that the Raman spectra *do* show exact isosbestic points, and that the previous data to the contrary were simply in error.<sup>15</sup> Moreover, the presently observed isosbestic

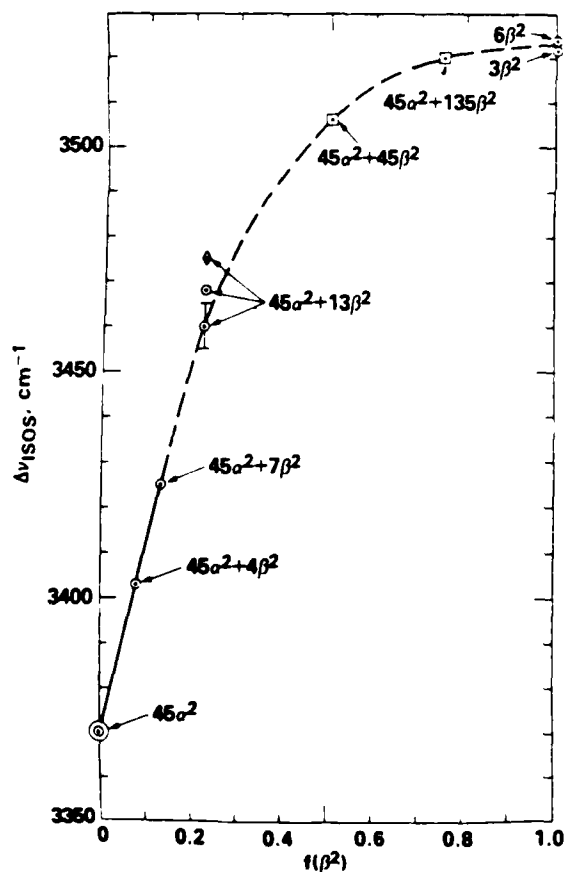


FIG. 7. The fraction of  $\beta^2$ ,  $f(\beta^2) = b/(a + b)$  (see the text) vs. the isosbestic frequency  $\Delta\nu_{\text{ISOS}}$  for the OH-stretching region from water between 3 and 85 °C. Circles, this work. Squares, calculated from the present data. Circle plus error bar, Ref. 12. Diamond, Ref. 15.

points are completely consistent with the spectroscopic mixture model of water, that is, the model in which two broad classes of interaction, HB and NHB, are in equilibrium, with the NHB class favored by rise of temperature.<sup>19</sup> Moreover, the various exact isosbestic frequencies observed here are totally unrelated to the continuum model. On the contrary, these points are solely the result of different linear combinations of  $\alpha^2$  and  $\beta^2$ . However, two of the isosbestic frequencies corresponding to the pure  $\alpha^2$  and pure  $\beta^2$  spectra relate to the spectroscopic mixture model in that they are thought to define the Gaussian component peak positions which separate the HB and NHB classes of OH oscillators in water.

The component peak positions and half-widths obtained by Walrafen<sup>23</sup> from Gaussian analysis were found to be essentially invariant for the  $3\beta^2$ ,  $45\alpha^2$ , and  $45\alpha^2 + 4\beta^2$  spectra from either H<sub>2</sub>O or D<sub>2</sub>O. However, the integrated Gaussian component intensities for the  $3\beta^2$  and  $45\alpha^2 + 4\beta^2$  spectra changed such that the intensity ratio of  $3\beta^2 / (45\alpha^2 + 4\beta^2)$  yielded component  $\rho$  values which agreed well between H<sub>2</sub>O and D<sub>2</sub>O. For all components, the integrated intensities scaled in the order  $3\beta^2$ ,  $45\alpha^2$ ,  $45\alpha^2 + 4\beta^2$ , with  $45\alpha^2 > 3\beta^2$  for highly polarized components, and  $45\alpha^2 > 3\beta^2$  for less strongly polarized components. This scaling is important in so far as it relates to invariance of the  $\Delta H^\circ$  obtained from the component data, as seen next.

Values of  $\Delta H^\circ$  for the HB→NHB equilibrium have been obtained from the temperature dependence of the NHB/HB Gaussian component intensity ratios.<sup>13,14</sup> Because the  $\Delta H^\circ$  value corresponds to the slope of plots of the NHB/HB intensity ratio vs  $T^{-1}$ , it is evident that no linear combination of  $3\beta^2$  or  $45\alpha^2$  can affect the  $\Delta H^\circ$  value, because the scaling between component intensities will not affect the slopes of the NHB/HB plots. Hence, no unique information related to the temperature dependence of the HB→NHB equilibrium can probably be obtained from use of any one linear combination of  $\alpha^2$  and  $\beta^2$  over any other, including pure  $\alpha^2$  and pure  $\beta^2$ .

#### IV. SUMMARY

Exact isosbestic points have been obtained in the Raman spectra from water between 3 and 85 °C. Isosbestic points from the pure  $\alpha^2$  and pure  $\beta^2$  spectra are thought to define the region of hydrogen-bonded and nonhydrogen-bonded interactions in water. Other isosbestic points which occur at intermediate frequencies simply arise from linear combinations of the  $\alpha^2$  or  $\beta^2$  spectra. No linear combination of  $\alpha^2$  or  $\beta^2$  gives special information about the temperature depen-

dence of the HB→NHB equilibrium in water over any other, including pure  $\alpha^2$  and pure  $\beta^2$ . The observed exactness of the isosbestic points constitutes strong evidence for a mixture model of water involving the general HB and NHB classes of OH oscillators. These classes, however, each encompass broad Gaussian components, and each Gaussian component refers to structures which involve a range of bond angles and distances distributed around the component peak position.

#### ACKNOWLEDGMENT

This work was supported by contracts from the Office of Naval Research.

- <sup>1</sup>E. B. R. Prideaux, *J. Soc. Chem. Ind.* **45**, 678 (1926), see p. 679 and Ref. 1.
- <sup>2</sup>W. R. Brode, *J. Am. Chem. Soc.* **46**, 581 (1924).
- <sup>3</sup>G. F. Bailey and R. J. Horvat, *J. Am. Oil Chem. Soc.* **49**, 494 (1972).
- <sup>4</sup>D. C. Harris, *Quantitative Chemical Analysis* (Freeman, New York, 1982), p. 494.
- <sup>5</sup>M. D. Cohen and E. Fischer, *J. Chem. Soc.* **1962**, 3044.
- <sup>6</sup>J. R. Morrey, *J. Phys. Chem.* **66**, 2196 (1962).
- <sup>7</sup>J. R. Morrey, *J. Phys. Chem.* **67**, 1569 (1963).
- <sup>8</sup>J. Brynestad and G. P. Smith, *J. Phys. Chem.* **72**, 296 (1968).
- <sup>9</sup>T. Nowicka-Jankowska, *J. Inorg. Nucl. Chem.* **33**, 2043 (1971).
- <sup>10</sup>D. V. Stynes, *Inorg. Chem.* **14**, 453 (1975).
- <sup>11</sup>J. D. Worley and I. M. Klotz, *J. Chem. Phys.* **45**, 2868 (1966).
- <sup>12</sup>G. E. Walrafen, *J. Chem. Phys.* **47**, 114 (1967).
- <sup>13</sup>G. E. Walrafen, *J. Chem. Phys.* **48**, 244 (1968).
- <sup>14</sup>G. E. Walrafen and L. A. Blatz, *J. Chem. Phys.* **59**, 2646 (1973).
- <sup>15</sup>J. R. Scherer, M. K. Go, and S. Kint, *J. Chem. Phys.* **78**, 1304 (1974).
- <sup>16</sup>G. d'Arrigo, G. Maisano, F. Mallamace, P. Miglardo, and F. Wanderlingh, *J. Chem. Phys.* **75**, 4264 (1981).
- <sup>17</sup>M. H. Brooker, in *The Chemical Physics of Solvation*, edited by J. Ulstrup *et al.* (Elsevier, Amsterdam, 1986).
- <sup>18</sup>These include the five orientations (abstract) plus the two orientations  $X(Z,X+Y)Y$  and  $X(Y,X+Z)Y$  without using a polarization scrambler.
- <sup>19</sup>G. E. Walrafen, M. R. Fisher, M. S. Hokmabadi, and W. -H. Yang, *J. Chem. Phys.* **85**, xxxx (1986).
- <sup>20</sup>*American Institute of Physics Handbook*, edited by D. E. Gray (McGraw-Hill, New York, 1957), pp. 6-90. The refractive index of water decreases from 1.3380 at 0 °C to 1.3270 at 80 °C for a wavelength of 486 nm.
- <sup>21</sup>Although most of the excitation from mercury lamps occurs at 90 deg, some of it involves angles ranging from ~20 to ~160 deg. Hence, an exact comparison between mercury and laser excitation is not possible, as pointed out by H. J. Bernstein (private discussions, 1974). Moreover, a polarization scrambler was not employed with the Cary 81 instrument, Ref. 12. Therefore, the present 8 cm<sup>-1</sup> agreement is satisfactory.
- <sup>22</sup>Measurements without a scrambler for the  $X(Z,X+Z)Y$  geometry indicate that the polarization response of the J. Y. gratings produces an abnormal enhancement of the strongly polarized OH-stretching regions. This effect is also present for the  $X(Y,X+Z)Y$  geometry. See Sec. II for isosbestic frequencies (unscrambled).
- <sup>23</sup>G. E. Walrafen, in *Structure of Water and Aqueous Solutions*, edited by W. A. P. Luck (Verlag Chemie, Weinheim, 1974).



Availability Codes		
Dist	Avail and/or Special	
A-1		

TECHNICAL REPORT DISTRIBUTION LIST, GEN

	<u>No. Copies</u>		<u>No. Copies</u>
Office of Naval Research Attn: Code 1113 800 N. Quincy Street Arlington, Virginia 22217-5000	2	Dr. David Young Code 334 NORDA NSTL, Mississippi 39529	1
Dr. Bernard Douda Naval Weapons Support Center Code 50C Crane, Indiana 47522-5050	1	Naval Weapons Center Attn: Dr. Ron Atkins Chemistry Division China Lake, California 93555	1
Naval Civil Engineering Laboratory Attn: Dr. R. W. Drisko, Code L52 Port Hueneme, California 93401	1	Scientific Advisor Commandant of the Marine Corps Code RD-1 Washington, D.C. 20380	1
Defense Technical Information Center Building 5, Cameron Station Alexandria, Virginia 22314	12 high quality	U.S. Army Research Office Attn: CRD-AA-IP P.O. Box 12211 Research Triangle Park, NC 27709	1
DTNSRDC Attn: Dr. H. Singerman Applied Chemistry Division Annapolis, Maryland 21401	1	Mr. John Boyle Materials Branch Naval Ship Engineering Center Philadelphia, Pennsylvania 19112	1
Dr. William Tolles Superintendent Chemistry Division, Code 6100 Naval Research Laboratory Washington, D.C. 20375-5000	1	Naval Ocean Systems Center Attn: Dr. S. Yamamoto Marine Sciences Division San Diego, California 91232	1

TECHNICAL REPORT DISTRIBUTION LIST, 051A

Dr. M. A. El-Sayed  
Department of Chemistry  
University of California  
Los Angeles, California 90024

Dr. E. R. Bernstein  
Department of Chemistry  
Colorado State University  
Fort Collins, Colorado 80521

Dr. J. R. MacDonald  
Chemistry Division  
Naval Research Laboratory  
Code 6110  
Washington, D.C. 20375-5000

Dr. G. B. Schuster  
Chemistry Department  
University of Illinois  
Urbana, Illinois 61801

Dr. J.B. Halpern  
Department of Chemistry  
Howard University  
Washington, D.C. 20059

Dr. M. S. Wrighton  
Department of Chemistry  
Massachusetts Institute of Technology  
Cambridge, Massachusetts 02139

Dr. A. Paul Schaap  
Department of Chemistry  
Wayne State University  
Detroit, Michigan 48207

Dr. W.E. Moerner  
I.B.M. Corporation  
Almaden Research Center  
650 Harry Rd.  
San Jose, California 95120-6099

Dr. A.B.P. Lever  
Department of Chemistry  
York University  
Downsview, Ontario  
CANADA M3J1P3

Dr. John Cooper  
Code 6173  
Naval Research Laboratory  
Washington, D.C. 20375-5000

Dr. George E. Walrafen  
Department of Chemistry  
Howard University  
Washington, D.C. 20059

Dr. Joe Brandelik  
AFWAL/AADO-1  
Wright Patterson AFB  
Fairborn, Ohio 45433

Dr. Carmen Ortiz  
Consejo Superior de  
Investigaciones Cientificas  
Serrano 121  
Madrid 6, SPAIN

Dr. John J. Wright  
Physics Department  
University of New Hampshire  
Durham, New Hampshire 03824

Dr. Kent R. Wilson  
Chemistry Department  
University of California  
La Jolla, California 92093

Dr. G. A. Crosby  
Chemistry Department  
Washington State University  
Pullman, Washington 99164

Dr. Theodore Pavlopoulos  
NOSC  
Code 521  
San Diego, California 91232

ATE  
LMED  
8